



Performance Evaluation of SPWM and SVPWM Inverter in FOC-based PMSM Drives Under Dynamic Speed and Load Disturbance

Mentari Putri Jati¹(✉) and Muhammad Rizani Rusli²

¹Department of Electro-optical Engineering, National Taipei University of Technology, Taiwan
t111999402@ntut.edu.tw

²Department of Electrical Engineering, Politeknik Elektronika Negeri Surabaya, Surabaya, Indonesia

Abstract. The article discusses the significance of high-performing Permanent Magnet Synchronous Motors (PMSM) in industries such as transportation, robotics, and industrial sectors due to their small size, high efficiency, and fast responsiveness. Field Oriented Control (FOC) is used in PMSM drives to achieve high-performance control of the motor by transforming three-phase AC currents and voltages into two orthogonal components. The article explains the two common Pulse Width Modulation (PWM) methods used in FOC PMSM drives: Sinusoidal PWM (SPWM) and Space Vector PWM (SVPWM). The paper evaluates the performance of FOC-based PMSM with inverter drives using SPWM and SVPWM under dynamic speed and load disturbance conditions to determine a reliable PWM inverter drive for PMSM FOC applications.

Keywords: Performance Evaluation, SPWM Inverter, SVPWM Inverter, FOC, PMSM Drives, Dynamic Speed, Load Disturbance

1 Introduction

Many industries, such as transportation, robotics, and industrial sectors, require high-performing Permanent Magnet Synchronous Motors (PMSM) that have a small size, high efficiency, fast responsiveness, and better control. These motors are compact, lightweight, less noisy, and fault-tolerant [1][3]. Due to manufacturer competition and applicable regulations, various equipment containing electric machines must meet new challenges of high performance, including dynamic speed control and robust load disturbance handling [4].

To achieve high-performance control of the motor, Field Oriented Control (FOC) is a popular technique used in PMSM drives. FOC works by transforming the three-phase AC currents and voltages of the motor into two orthogonal components: a direct current component and a quadrature current component. By controlling these two components, the torque and speed of the motor can be controlled precisely. The PMSM application uses a resolver for rotor position sensing, which is mounted mechanically on the motor

shaft and operates properly by utilizing electromagnetic induction. The analog signals from the coils are converted into a digital signal form to be used for commutation in a three-phase inverter using a resolver to digital converter. [5].

There are two common Pulse Width Modulation (PWM) methods used in FOC PMSM drives: Sinusoidal PWM (SPWM) and Space Vector PWM (SVPWM). SPWM is a simple method that generates a sinusoidal waveform at the desired frequency and amplitude to control the motor. SVPWM, on the other hand, is a more advanced method that generates a voltage vector that follows the desired trajectory in the voltage space vector diagram. SVPWM provides better utilization of the DC bus voltage and reduces harmonic distortion [6], [7].

This paper discusses the performance evaluation of FOC-based PMSM with inverter drives using SPWM and SVPWM. The tests are carried out under dynamic speed conditions and load disturbance conditions to prove the reliability of the controller through a PSIM environment. The purpose of this performance evaluation is to determine a reliable PWM inverter drive for PMSM FOC applications.

2 Method

2.1 Field Oriented Permanent Magnet Synchronous Motor (PMSM) Control

Field-oriented control (FOC) has been widely adopted by researchers in PMSM velocity control because it is an effective technique. To produce smooth torque and reduce power loss, vibration, and noise in PMSM mode of operation, the current waveform should match the shape of the back EMF of a sinusoidal motor [8]. Therefore, high resolution rotor position feedback is important. On the other hand, accurate speed tracking requires speed feedback.

The block diagram of the system is shown in Fig. 1. The speed reference parameter referred to in the block diagram below is the input speed setpoint value for the motor. There is feedback in the form of a speed sensor to be compared with a reference speed. Comparison between speed reference and speed will produce an error as input to the PI controller.

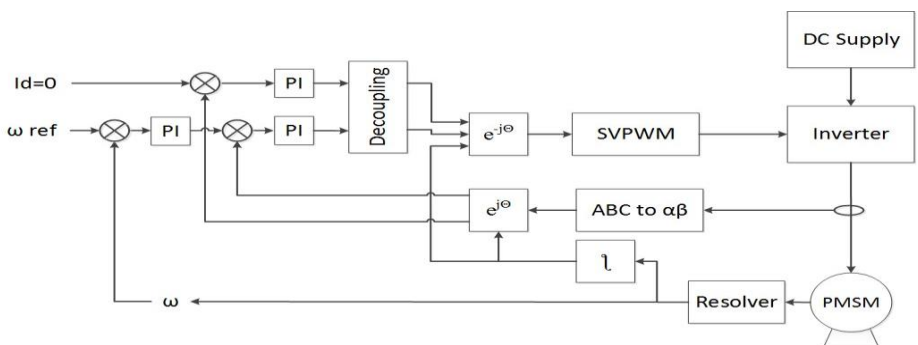


Fig. 1. Field Oriented Permanent Magnet Synchronous Motor (PMSM) Control Diagram Block

2.2 Space Vector Pulse Width Modulation (SVPWM)

To generate a sinusoidal waveform of the three-phase output voltage in SVPWM, the correct switching combination of the three-phase inverter is determined, and the on-off time duration of the switching is calculated. Voltage space vectors represent SVPWM switching combinations. These vectors are selected to approximate the reference voltage vector with the desired frequency and amplitude within a small time interval. As the reference stress vector rotates to a new angular position, a new set of stationary stress vectors is selected. By sequentially sampling the complete cycle of the desired voltage vector, the average output voltage duplicates the reference voltage. In addition to providing the desired phase shift between the input voltage and current, the chosen vector must minimize switching losses and obtain the desired output current or voltage while minimizing Total Harmonic Distortion (THD)[9].

The operating principle of the SVPWM will be illustrated by the hexagonal vector approximation of the output voltage and input current shown in Fig. 2. To calculate the amplitude and reference angle, the three-phase magnitude is transformed into the two-phase alpha-beta axis. These values are then grouped into six voltage and current vectors, which are used to determine the amplitudes and angles in each sector. Based on the sector value, the switches are turned on and off to satisfy the given voltage and current vectors. This helps in minimizing switching losses in the power converter by efficiently determining the switch combinations in each sector [10], [11].

$$\begin{aligned}
 C_1 &= 1 - C_4 \\
 C_2 &= 1 - C_5 \\
 C_3 &= 1 - C_6
 \end{aligned}
 \tag{1}$$

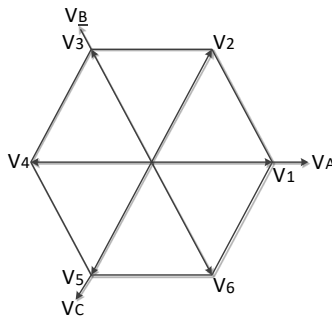


Fig. 2. Hexagon Voltage Vector

From equation 1, the inverter voltage output is of the following equation below [10], [11].

$$\begin{bmatrix} Va \\ Vb \\ Vc \end{bmatrix} = \frac{V_{dc}}{3} \begin{bmatrix} 2 & -1 & -1 \\ -1 & 2 & -1 \\ -1 & -1 & 2 \end{bmatrix} \begin{bmatrix} C1 \\ C2 \\ C3 \end{bmatrix} \quad (2)$$

$$V_s = V_a + jV_\beta = \sqrt{\frac{2}{3}} \left(V_a + V_\beta e^{j\frac{2\pi}{3}} + V_\beta e^{j\frac{4\pi}{3}} \right) \quad (3)$$

To calculate the duty cycle ratio configuration, a similar procedure for the other component vectors can be used. The switching determination vectors for all input and output sectors can be determined using 27 combinations. It is important to note that the duty cycle ratio configuration must have a positive value.

3 Result and Discussion

3.1 Constant Speed No Load

To evaluate the drives system of a PMSM, a comparative simulation of two modulation techniques: SPWM and SVPWM was carried out using PSIM environment with various conditions where system parameters are shown in Table 1. Speed response, current, torque ripple, and Total Harmonic Distortion (THD) will be analyzed. The simulation is carried out at constant and dynamic speed with and without load.

Table 1. PMSM Parameters

Parameter	Value
Rs (stator resistance)	4.3 W
Ld (d-axis inductance)	27mH
Lq (q-axis inductance)	67mH
Vpeak / krpm	98.67
No. of poles	4
Moment of inertia	1.79m

The response output with a speed set point of 3000 Rpm No load is shown in Fig. 3. Fig. 3 a shows that the closed loop system can follow the PMSM constant speed set point using two different types of modulation. For all the simulation results, SVPWM graphic results use the orange line, SPWM blue line, and the reference speed uses the red line. The current response and torque ripple are shown in Figure 3b. Figure 3c shows the torque ripple and starting overshoot of SVPWM are lower than SPWM.

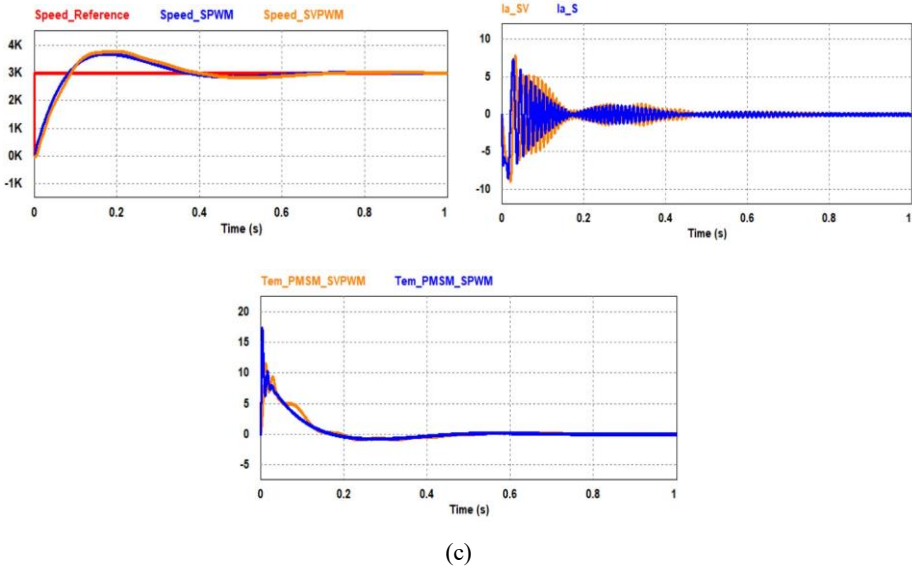


Fig. 3. Permanent Magnet Synchronous Motor (PMSM) Performance at Constant Speed 3000 RPM No Load. (a) Speed Response (b) Current (c) Torque

3.2 Constant Speed with Constant Load

The system performance responds with the constant speed with the constant load as shown in Fig. 4 with an installed load of 4 Nm. At a constant speed of 3000 Rpm, the speed response is shown in Fig. 4a for a 4 Nm load. Meanwhile, the current graphs are shown in Fig. 4b with an explanation of the THD values in Fig. 4c. SVPWM THD is lower than SPWM with different loads. The current spectrum is shown in Fig. 4d. Fig. 4e show the torque ripple response of each modulation technique.

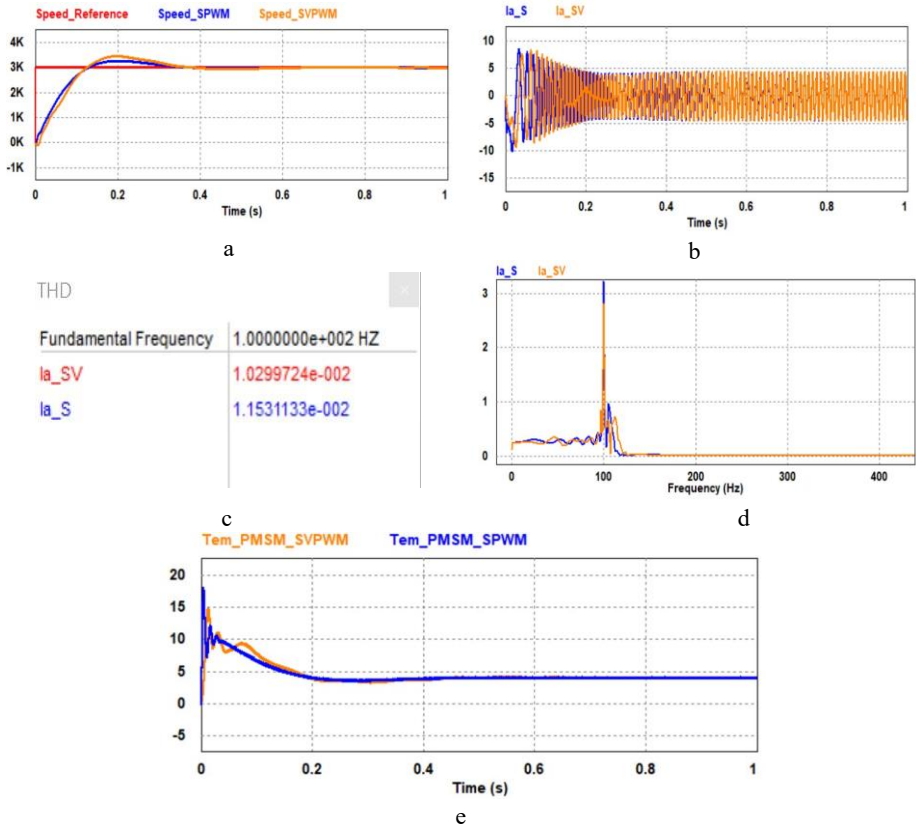


Fig. 4. PMSM Performance at Constant Speed 3000 RPM With 4 Nm Load. (a) Speed Response (b) Current (c) THD (d) Current Spectrum (e) Torque Ripple

3.3 Dynamic Speed with and Without Constant Load

The system performance responds with the dynamic speed with the constant load as shown in Fig. 5 with an installed load of 4 Nm and 2 Nm. At a constant speed of 3000 Rpm, the speed graph is shown in Fig. 5a for a 4 Nm load and Fig. 5f for a 2 Nm load. The dynamic speed setpoint starts at 3000 Rpm, 2000 Rpm, and 1000 Rpm and returns to 3000 Rpm.

The current graphs are shown in Fig. 5b and Fig. 5g where the average amplitude is greater at 2 Nm installed load than at 4 Nm load. The THD value of the system is shown in Fig. 5c and Fig. 5h. SVPWM THD is lower than SPWM with different loads. The current spectrum is shown in Fig. 5d and Fig. 5i while Fig. 5e and Fig. 5j show the torque ripple response.

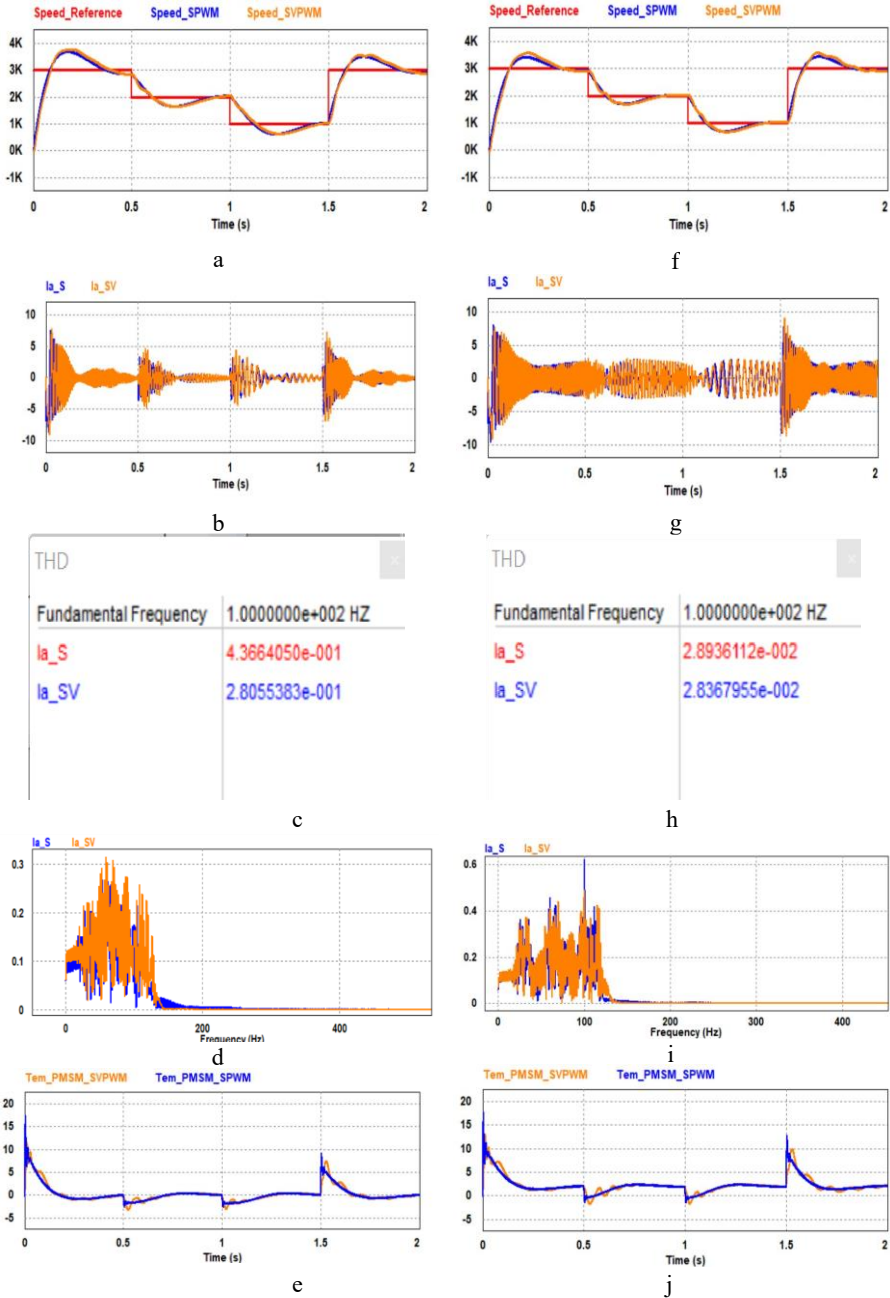


Fig. 5. PMSM Performance at Dynamic Speed No Load and With Load. (a) Speed Response No Load (b) Current No Load (c) THD No Load (d) Current Spectrum No Load (e) Torque Ripple No Load (f) Speed Response 2 Nm Load (g) Current 2 Nm Load (h) THD 2 Nm Load (i) Current Spectrum 2 Nm Load (j) Torque Ripple 2 Nm Load

3.4 Constant Speed with Load Disturbance

Load changes can have a negative impact on motor performance, so the proposed system was tested with load changes as a disturbance to verify its reliability. Fig. 6 shows that the system responds with constant speed even when there is a load disturbance. The load changes from 2 Nm between 0-1 seconds to 4 Nm between 1-1.5 seconds and then back to 2 Nm. The speed graph in Fig. 6a shows that the system experiences overshoot when the load changes, but maintains a constant speed of 3000 RPM.

The current graph is shown in Fig. 6b which increases in amplitude when the load changes by 2 Nm. The system THD value is shown in Fig. 6c where the SVPWM THD is lower than SPWM. The current spectrum and torque ripple response are shown in Fig. 6d and Fig. 6e.

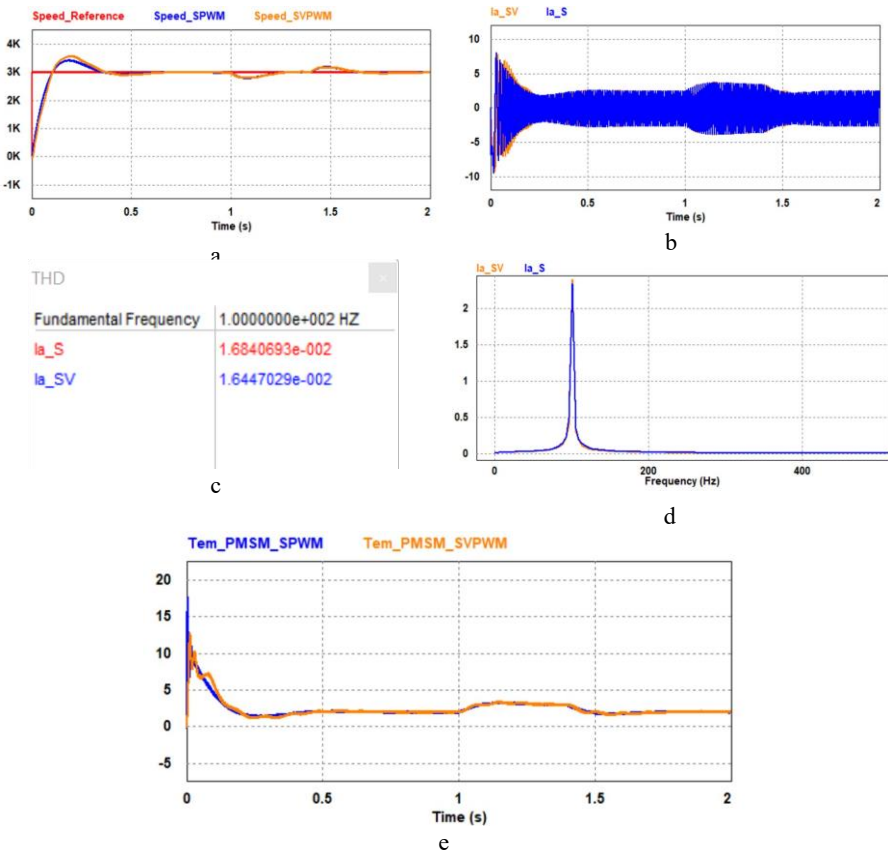


Fig. 6. PMSM Performance at Constant Speed With Load Disturbance. (a) Speed Response (b) Current (c) THD (d) Current Spectrum (e) Torque Ripple

4 Conclusion

A performance simulation evaluation of two modulation techniques, SPWM and SVPWM, was conducted to evaluate the drives system of a PMSM under various conditions. The simulation was carried out at constant and dynamic speed with and without load to analyze speed response, current, torque ripple, and Total Harmonic Distortion (THD). Results showed that SVPWM had lower torque ripple and THD values than SPWM under different load conditions. Furthermore, the SVPWM demonstrated its reliability in maintaining a constant speed even with load disturbances. Overall, SVPWM showed better performance compared to SPWM in terms of current response, torque ripple, and THD.

References

1. O. Saadaoui, A. Khlaief, M. Abassi, I. Tlili, A. Chaari, and M. Boussak, "A New FullOrder Sliding Mode Observer Based Rotor Speed and Stator Resistance Estimation for Sensorless Vector Controlled PMSM Drives," *Asian J Control*, vol. 21, no. 3, pp. 1318–1327, May 2019.
2. M. T. Kassa and D. Changqing, "Design Optimazation and Simulation of PMSM based on Maxwell and TwinBuilder for EVs," in *2021 8th International Conference on Electrical and Electronics Engineering, ICEEE 2021*, Apr. 2021, pp. 99–103.
3. J. Dilys, "Modeling of Sensorless Control of Permanent-Magnet Synchronous Motors," 2020.
4. E. Purwanto, M. Putri Jati, B. Sumantri, and M. Rizani Rusli, "Performance Enhancement of Matrix Converter Fed Induction Motor Drives Using Fuzzy Supervisory Controller," in *IES 2020 - International Electronics Symposium: The Role of Autonomous and Intelligent Systems for Human Life and Comfort*.
5. M. R. Rusli *et al.*, "Digital Implementation of Space Vector PWM for Three Phase Inverter with Simplified C-Block PSIM Utilization," in *International Electronics Symposium 2021: Wireless Technologies and Intelligent Systems for Better Human Lives, IES 2021 - Proceedings*, 2021.
6. M. P. Jati *et al.*, "A fuzzy supervisory scalar control for matrix converter induction motor drives," *International Journal on Electrical Engineering and Informatics*, vol. 13, no. 1, 2021.
7. L. Xiao, J. Li, J. Chen, R. Qu, and Y. Xiong, "Synchronous SVPWM for Field-oriented Control ofPMSM Using Phase-lock Loop," in *IEEE Energy Conversion Congress & Expo*, 2017, pp. 4324–4331.
8. M. Hasoun, A. el Afia, and M. Khafallah, "Field Oriented Control of Dual Three-Phase PMSM Based Vector Space Decomposition for Electric Ship Propulsion," in *International Conference of Computer Science and Renewable Energies*, 2019, pp. 1–6.
9. M. Khan, W. Yong, and E. Mustafa, "Design and Simulation of Control Technique for Permanent Magnet Synchronous Motor Using Space Vector Pulse Width Modulation," in *IOP Conference Series: Materials Science and Engineering*, Aug. 2017, vol. 224, no. 1.
10. M. Abassi, A. Khlaief, O. Saadaoui, A. Chaari, and M. Boussak, "Performance Analysis of FOC and DTC for PMSM Drives using SVPWM Technique," in *international conference*

on Sciences and Techniques of Automatic control & computer engineering, 2015, pp. 228–233.

11. M. Abassi, O. Saadaoui, I. Tlili, A. Khlaief, A. Chaari, and M. Boussak, “PMSM DTC Drive System Fed by Fault-Tolerant Inverter Connected to a Photovoltaic Source,” in *International Renewable Energy Congress*, 2018.

Open Access This chapter is licensed under the terms of the Creative Commons Attribution-NonCommercial 4.0 International License (<http://creativecommons.org/licenses/by-nc/4.0/>), which permits any noncommercial use, sharing, adaptation, distribution and reproduction in any medium or format, as long as you give appropriate credit to the original author(s) and the source, provide a link to the Creative Commons license and indicate if changes were made.

The images or other third party material in this chapter are included in the chapter's Creative Commons license, unless indicated otherwise in a credit line to the material. If material is not included in the chapter's Creative Commons license and your intended use is not permitted by statutory regulation or exceeds the permitted use, you will need to obtain permission directly from the copyright holder.

